

This is a repository copy of *Doubling fusion power with volumetric optimization in magnetic confinement fusion devices*.

White Rose Research Online URL for this paper:

<https://eprints.whiterose.ac.uk/223163/>

Version: Published Version

Article:

Parisi, J.F., Berkery, J.W., Sladkomedova, Alsu orcid.org/0000-0002-0012-9328 et al. (17 more authors) (2025) Doubling fusion power with volumetric optimization in magnetic confinement fusion devices. *Physical Review Research*. 013139. ISSN 2643-1564

<https://doi.org/10.1103/PhysRevResearch.7.013139>

Reuse

This article is distributed under the terms of the Creative Commons Attribution (CC BY) licence. This licence allows you to distribute, remix, tweak, and build upon the work, even commercially, as long as you credit the authors for the original work. More information and the full terms of the licence here:

<https://creativecommons.org/licenses/>

Takedown

If you consider content in White Rose Research Online to be in breach of UK law, please notify us by emailing eprints@whiterose.ac.uk including the URL of the record and the reason for the withdrawal request.

Doubling fusion power with volumetric optimization in magnetic confinement fusion devices

J. F. Parisi ^{1,*}, J. W. Berkery ¹, A. Sladkomedova ², S. Guizzo ³, M. R. Hardman,² J. R. Ball ⁴, A. O. Nelson ³, S. M. Kaye ¹, M. Anastopoulos-Tzanis ², S. A. M. McNamara ², J. Dominski ¹, S. Janhunen,² M. Romanelli,² D. Dickinson ⁵, A. Diallo,¹ A. Dnestrovskii ², W. Guttenfelder ^{6,1}, C. Hansen ³, O. Myatra ⁷ and H. R. Wilson⁸

¹Princeton Plasma Physics Laboratory, Princeton University, Princeton, New Jersey 08540, USA

²Tokamak Energy Ltd., 173 Brook Drive, Milton Park, Oxfordshire OX14 4SD United Kingdom

³Department of Applied Physics & Applied Mathematics, Columbia University, New York, 10027 New York, USA

⁴Ecole Polytechnique Federale de Lausanne, Swiss Plasma Center, Lausanne CH1015, Switzerland

⁵York Plasma Institute, Department of Physics, University of York, Heslington, York YO10 5DQ, United Kingdom

⁶Type One Energy, 8383 Greenway Boulevard, Middleton, Wisconsin 53562, USA

⁷United Kingdom Atomic Energy Authority, Culham Science Centre, Abingdon OX14 3DB, United Kingdom

⁸Oak Ridge National Laboratory, Oak Ridge, Tennessee 37830, USA



(Received 17 April 2024; accepted 4 January 2025; published 7 February 2025)

A technique, volumetric power optimization, is presented for enhancing the power output of magnetic confinement fusion devices. Applied to a tokamak, this approach involves shifting the burning plasma region to a larger plasma volume while introducing minimal perturbations to the plasma boundary shape. This edge perturbation—squareness—is analogous to pinching and stretching the edge boundary. Stability calculations confirm that this edge alteration is compatible with maintaining plasma stability. This optimization method for optimizing fusion power output could improve the performance of magnetic confinement fusion power plants.

DOI: [10.1103/PhysRevResearch.7.013139](https://doi.org/10.1103/PhysRevResearch.7.013139)

I. INTRODUCTION

The variation of fusion power in a power plant is a complex issue, and is one of the primary, if not the primary, cost drivers of a fusion power plant [1]. In this article, we introduce a technique for optimizing fusion power through the volumetric distribution of the magnetic equilibrium [2,3]. This approach substantially increases the power output of magnetic confinement systems while enabling variable-power operation, addressing challenges in the practical deployment of fusion energy.

The relationship between total thermal fusion power and net power output in fusion power plants is highly nonlinear: increases in thermal power lead to disproportionately large increases in net power output due to recirculating power to plant systems [4–6]. As such, strategies that increase total fusion power without raising recirculating power are highly desirable. Furthermore, as electric grids increasingly integrate variable renewable energy sources, the ability of baseload power plants to provide variable power output becomes increasingly valuable [7–9]. This trend is reflected in modern fission reactor designs, which offer variable output options despite their historical reliance on fixed operation [10–13].

In this work, we focus on tokamaks, the leading candidate for commercial fusion energy. Tokamaks confine deuterium-tritium (DT) plasma within a magnetic cage. We show that small adjustments to the magnetic cage shape can significantly increase total fusion power. This capability not only enhances the flexibility of tokamaks but could also substantially reduce the capital cost of fusion power plants [1]. While various methods for varying power output have been proposed—such as adjusting the fuel mix [14–16], density profiles [17], or total plasma volume—each presents significant physics and engineering challenges. For example, increasing fueling rates can impact plasma performance in several ways: exceeding density limits can trigger instabilities [18–20], modifying the bootstrap current profiles can alter confinement properties [21–23], and reshaping heating and fueling deposition profiles can affect energy distribution [24–26]. Similarly, adjusting the DT fuel mix [14,27] can degrade plasma performance due to isotope effects, which influence transport and stability properties [28–31]. The approach we present offers a promising alternative solution with lower complexity.

We demonstrate the potential of volumetric optimization in an example with plasma squareness. By varying the plasma edge squareness, ζ_0 , we demonstrate simultaneous achievement of high maximum fusion power and flexibility to control the fusion burn with minimal disruption to the overall plasma configuration. Increasing ζ_0 redistributes plasma volume to regions of higher power density, leading to significant increases in fusion power. This approach is operationally advantageous as it allows key plasma parameters, such as elongation and triangularity, to remain unchanged while squareness is

*Contact author: jparisi@pppl.gov

Published by the American Physical Society under the terms of the [Creative Commons Attribution 4.0 International](https://creativecommons.org/licenses/by/4.0/) license. Further distribution of this work must maintain attribution to the author(s) and the published article's title, journal citation, and DOI.

adjusted. Although this work focuses on plasma squareness, it represents just one application of volumetric optimization.

II. VOLUMETRIC POWER OPTIMIZATION

Magnetic confinement schemes must confine plasma at sufficient pressure for a high fusion power density p_f . However, high p_f is insufficient for substantial fusion power; it must also persist over a large fraction of the total plasma volume V_{tot} . The largest contributions to the total fusion power

$$P_f = \int p_f dV, \quad (1)$$

come from the burn volume

$$V_{\text{burn}} \equiv \int_{\text{burn}} dV, \quad (2)$$

the volume over which p_f exceeds a value $p_{f,c}$ required for substantial fusion power. We use $p_{f,c} = 1 \text{ MW/m}^3$, which is justified later. In this work, we control P_f by changing the fraction of the total plasma volume V_{tot} packed into V_{burn} , given by the packing number

$$\Pi \equiv V_{\text{burn}}/V_{\text{tot}}. \quad (3)$$

Plasmas with $\Pi = 1$ are volume efficient, packing the full volume into power dense regions. In contrast, $\Pi = 0$ is volume inefficient since $V_{\text{burn}} = 0$. Thus, at fixed V_{tot} ,

$$P_f \sim \Pi \langle p_f \rangle_{\text{burn}}, \quad (4)$$

where the burn average $\langle \cdot \rangle_{\text{burn}}$ is

$$\langle p_f \rangle_{\text{burn}} \equiv (1/V_{\text{burn}}) \int_{\text{burn}} p_f dV. \quad (5)$$

The key idea of this work is that total fusion power can be significantly increased by maximizing Π in Eq. (3), corresponding to an efficient use of the plasma volume. In this paper, we demonstrate how to vary Π using plasma squareness. Adjusting the plasma edge squareness [32],

$$\zeta_0 = \arcsin(Z_m/\kappa_0 a) - \pi/4, \quad (6)$$

changes Π , and thus P_f , while $\langle p_f \rangle_{\text{burn}}$ is approximately constant according to infinite- n ballooning stability [33–35], which we explain in a later section. Here, Z_m is the Z value indicated by crosses in Fig. 1 inset and $\kappa_0 = h/2a$ is the edge plasma elongation where h is the maximum plasma height and a is the minor radius. By maximizing Π in Eq. (4) using squareness, the fusion power increases significantly.

Dedicated studies of plasma squareness are limited compared with other shape parameters, but benefits to increased ζ_0 have been identified. Squareness control is established [32,36–39] and less disruptive than other shape parameters because plasma x points and maximum width and height can be fixed. Ion-scale turbulence simulations found that higher ζ_0 improves heat confinement [40], and DIII-D and MAST-U experiments show ζ_0 values typically allow higher edge plasma pressure [41–45] and give improved core confinement [46]. Spherical tokamak design studies found positive moderate ζ_0 stabilized kink modes, allowing a 10% increase in core plasma pressure [32,47,48]. This benefit was discounted because of the required increase in poloidal field coil current [48,49], but

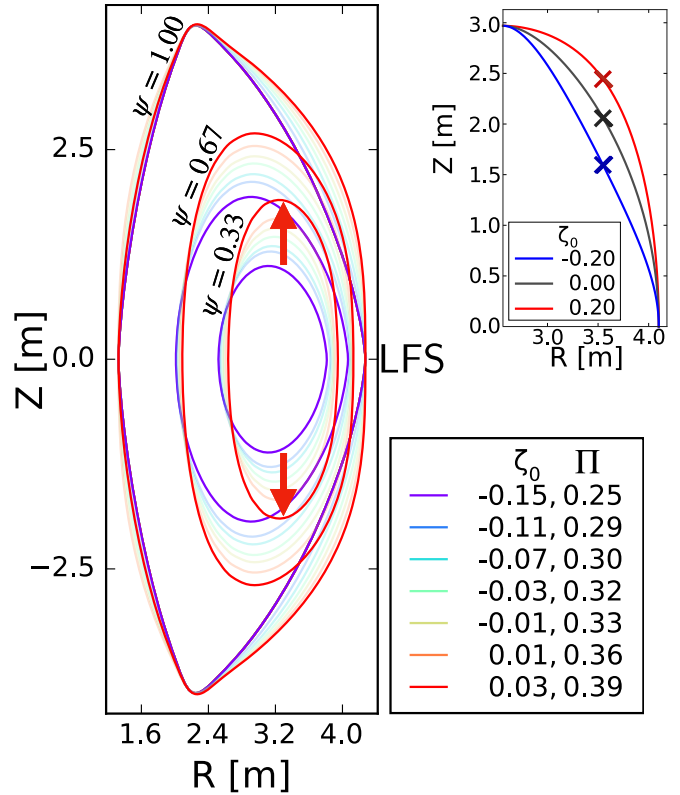


FIG. 1. Main: three flux surfaces $\psi = [0.33, 0.67, 1.0]$ with varying edge squareness ζ_0 and Π . Red arrows show stretching of inner flux surfaces by increasing ζ_0 . Inlet: outer flux surfaces for three ζ_0 values.

the benefits outlined in this work could change that tradeoff assessment. Furthermore, the poloidal coil currents required for the equilibria in this study are probably easier to handle since we examine significantly lower ζ_0 values. It should be noted that changes to parameters like κ_0 or ζ_0 may require changes in other plasma parameters, such as internal inductance [4]. The work in this study is based on a representative burning spherical tokamak [50] design point, referred to as GST. The main GST parameters are on-axis toroidal field $B_{T,0} = 5\text{T}$, plasma current $I_p = 9.8\text{MA}$, major radius $R_0 = 3.4\text{m}$, $a = 1.5\text{m}$, $\kappa_0 = 2.73$, and triangularity $\delta_0 = 0.43$.

III. SQUARENESS

Increasing squareness of the plasma edge stretches the magnetic surfaces in the plasma core. An equilibrium with $\zeta_0 = 0.03$ has core flux surfaces that are twice as elongated as a lower ζ_0 equilibrium with $\zeta_0 = -0.15$. This is illustrated in Fig. 1—we plot surfaces of constant normalized poloidal flux ψ with different ζ_0 and almost constant plasma volume. Comparison of the inner $\psi = 0.33$ flux surfaces for $\zeta_0 = -0.15$ and $\zeta_0 = 0.03$ shows that higher ζ_0 elongates the plasma core.

Increased core elongation more efficiently uses the core volume for fusion power by increasing V_{burn} and hence $\Pi \sim \langle \kappa \rangle_{\text{burn}}$. The total power is therefore determined mainly by p_f

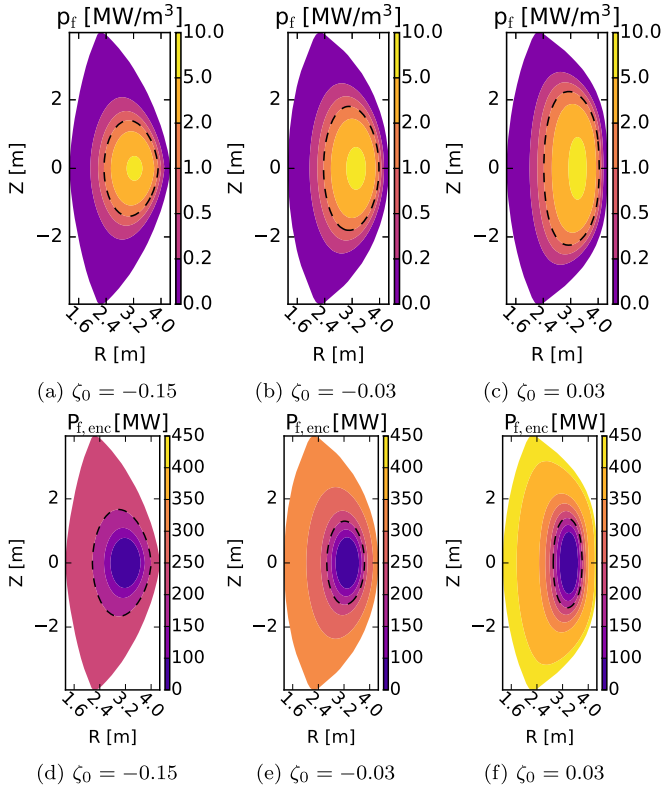


FIG. 2. Burn control scheme using plasma squareness for GST: Fusion power density (a)–(c) and enclosed fusion power (d)–(f) in increasingly square plasmas. The $p_f = 1 \text{ MW/m}^3$ and $P_f = 200 \text{ MW}$ surfaces are indicated with a dashed black contour. The total fusion power is 215 MW, 311 MW, and 403 MW for $\zeta = -0.15, -0.03$, and 0.03.

and κ in the burn region,

$$P_f \sim \langle \kappa \rangle_{\text{burn}} \langle p_f \rangle_{\text{burn}}, \quad (7)$$

for fixed V_{tot} . Therefore, ζ_0 , mainly through $\langle \kappa \rangle_{\text{burn}}$, determines Π and thus the fusion burn.

The physical mechanism for ζ_0 increasing Π exploits plasma properties at the low-field side (LFS), indicated in Fig. 1. With increasing plasma squareness, Π increases from 0.25 to 0.39, shown in Fig. 1. The strong poloidal field at the LFS causes LFS flux surfaces to be closely spaced, measured by large $|d\psi/dr|_{\text{LFS}}$ values, where r is the plasma minor radial coordinate. When ζ_0 increases, flux surfaces in the plasma core are stretched vertically in order to keep $|d\psi/dr|_{\text{LFS}}$ large, indicated by red arrows in Fig. 1. This effect increases for spherical tokamaks where the LFS poloidal field is particularly strong [50] and for high Shafranov shift [51], which both increase $|d\psi/dr|_{\text{LFS}}$.

The total power P_f doubles from the minimum to maximum ζ_0 values, from $P_f = 215 \text{ MW}$ to 403 MW. The corresponding p_f is plotted for plasmas with three ζ_0 values in Figs. 2(a)–2(c). The highest ζ_0 equilibrium has p_f surfaces that are much more elongated [Fig. 3(b)] and it therefore has a high Π value ($\Pi = 0.39$ compared with $\Pi = 0.25, 0.32$ for $\zeta_0 = -0.15, -0.03$). Thus, higher ζ_0 equilibria efficiently distribute volume to regions of high $p_f(\psi)$, which increases P_f ,

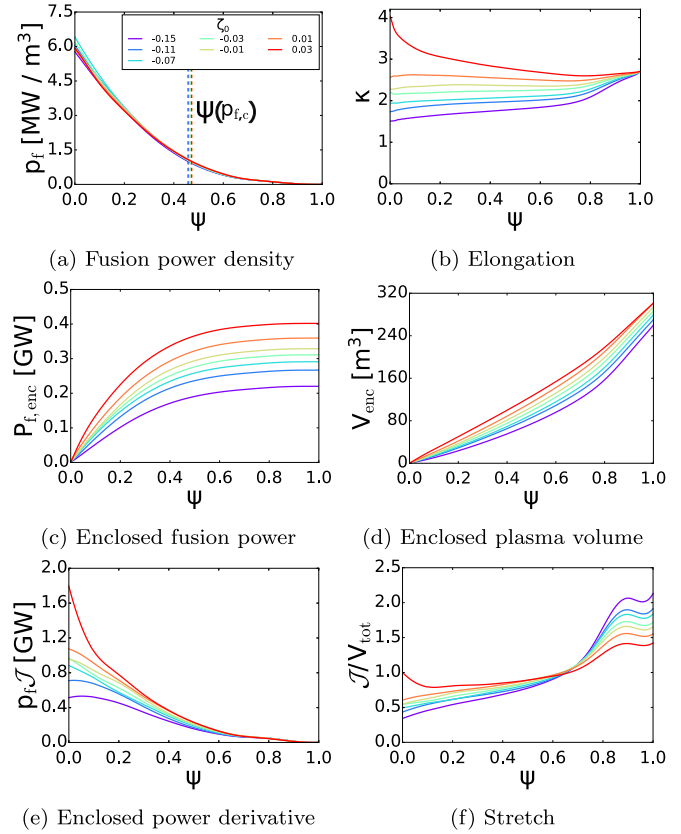


FIG. 3. GST radial profiles of power density (a), elongation (b), enclosed power (c), enclosed volume (d), and enclosed power derivative [Eq. (9)] (e), and Stretch [Eq. (10)] (f).

despite similar $p_f(\psi)$ profiles [Fig. 3(a)]. For example, for $\zeta_0 = 0.03$ the flux surface $\psi = 0.2$ has an enclosed power

$$P_{f,\text{enc}}(\psi) \equiv \int_0^{V(\psi)} p_f dV' \quad (8)$$

of 231 MW, but $\zeta_0 = -0.15$ has only 98 MW [Figs. 2(d)–2(f) and 3(c)]. In Fig. 3(a), vertical lines indicate the surface ψ_{burn} where $p_{f,c} = 1 \text{ MW/m}^3$; for all equilibria, $P_{f,\text{enc}}(\psi_{\text{burn}})/P_f > 90\%$, indicating a good choice of $p_{f,c}$.

Higher ζ_0 equilibria enclose more fusion power by growing volume relatively quickly in the burn region but slowly outside. The Jacobian $\mathcal{J} = dV_{\text{enc}}/d\psi$ measures flux-surface growth for enclosed volume $V_{\text{enc}}(\psi) \equiv \int_0^{V(\psi)} dV'$ [Fig. 3(d)]. \mathcal{J} enters the derivative of $P_{f,\text{enc}}$,

$$dP_{f,\text{enc}}/d\psi = p_f \mathcal{J}, \quad (9)$$

so larger \mathcal{J} indicates faster flux-surface volume growth, contributing more to P_f . Average contributions to P_f in the burn region are double for the highest ζ_0 than the lowest ζ_0 , shown by $p_f \mathcal{J}$ in Fig. 3(e). This explains how the highest ζ_0 has double the P_f of the lowest ζ_0 . The Stretch S is the normalized rate of volume growth,

$$S = \mathcal{J}/V_{\text{tot}}, \quad (10)$$

satisfying $\int_0^1 S d\psi = 1$. Surfaces with $S > 1$ increase volume faster than the average flux surface and those with

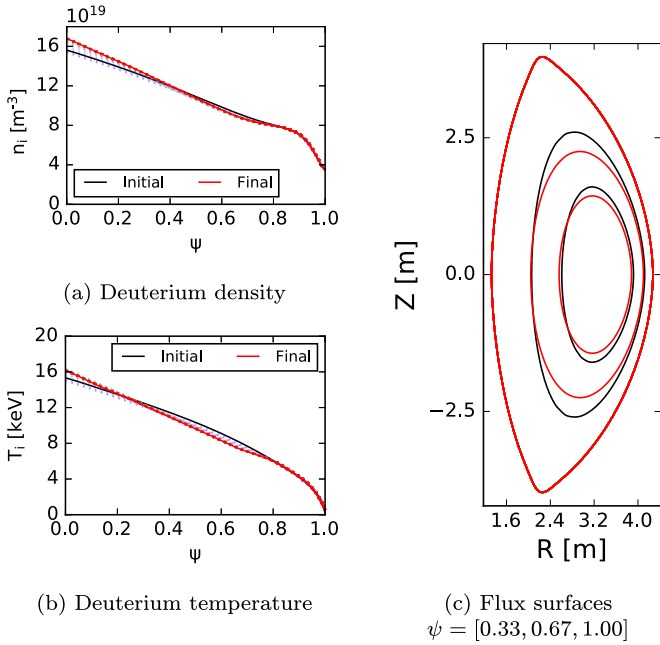


FIG. 4. Initial and final ion density and temperature for GST [(a), (b)], and equilibria (c) for $\zeta_0 = -0.01$. In (a) and (b), dotted lines are intermediate iterations. The final profile is infinite- n ballooning stable.

$S < 1$ increase volume slower than average. Because $S \sim (\kappa/\kappa_0)(r/a)(B_{p,0}/B_p)$, where $B_{p,0}$ is the edge poloidal field, we expect $S \ll 1$ near the core but $S \gg 1$ at the edge. This is true for low ζ_0 equilibria, shown in Fig. 3(f), but for high ζ_0 equilibria, $S \approx 1$ in V_{burn} , and increases slowly near the edge. Therefore, high ζ_0 equilibria expand plasma volume relatively quickly in the burn region, whereas low ζ_0 equilibria expand plasma volume relatively quickly in the edge where p_f is low.

IV. EQUILIBRIUM GENERATION

While this paper’s focus is on geometry insights and not integrated modeling, we ensure that the equilibria presented here clear a minimum threshold for viability: infinite- n ballooning stability [33–35], which is an approximation for kinetic-ballooning-mode stability [52,53]. We found that changing the equilibrium magnetic geometry by varying ζ_0 but keeping the profiles fixed caused some equilibria to be ballooning unstable. Therefore, for a fair comparison across ζ_0 values, we use an iterative scheme that generates equilibria close to the infinite- n ballooning stability boundary. For each iteration, at ten radial locations the density and temperature gradients for thermal species are brought to the ballooning stability boundary. The fixed-boundary equilibrium is recalculated using CHEASE [54] according to the new pressure and current profiles (with consistent bootstrap current [55,56]), subject to keeping the total plasma current I_p fixed. Increasing ζ_0 also increases the bootstrap fraction f_{bs} from $f_{\text{bs}} = 0.72$ to $f_{\text{bs}} = 0.96$ for the lowest to the highest ζ_0 . The strong increase in f_{bs} results from increased core elongation at higher ζ_0 [57]. The equilibria have five thermal species—deuterium, tritium, lithium, helium, and electrons—and a fast helium population. In Fig. 4(a) and 4(b), we plot the deuterium

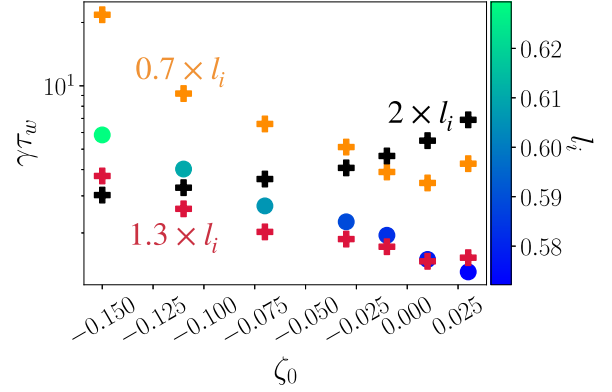


FIG. 5. Vertical stability growth rates $\gamma\tau_w$ across squareness for GST for nominal l_i (circles) and rescaled l_i (pluses).

temperature and density at each iteration step, and in Fig. 4(c) flux surfaces for the initial and final equilibria. To simplify analysis, we present results with fixed pressure in the pedestal edge region. Because of the effect of shape on pedestal performance [41,58–60], we performed sensitivity analysis that showed the trends in this work still held with different pedestal heights.

V. VERTICAL STABILITY

High plasma elongation can make a plasma more vertically unstable and trigger violent plasma termination events [61–66]. Thus, it is important to determine how ζ_0 and its strong effects on $\langle\kappa\rangle_{\text{burn}}$ [Fig. 3(b)] affect vertical stability (VS). To assess VS, we use Tokamak [67] to find VS growth rates for equilibria with different ζ_0 values. Free-boundary equilibria were generated and the VS growth rate $\gamma\tau_w$ calculated for the $n = 0$ mode, where the growth rate γ is normalized to the wall resistive time τ_w and n is the toroidal mode number. Shown in Fig. 5, at the nominal inductance l_i values, $0.57 < l_i < 0.63$, increasing ζ_0 is stabilizing. We rescaled l_i by factors of 0.7, 1.3, and 2.0, finding that slightly higher l_i was stabilizing, but much higher and lower l_i became destabilizing. We hypothesize ζ_0 stabilization at nominal l_i values is due to a larger Shafranov shift at higher squareness, leading to stronger plasma-wall coupling. At higher l_i , the Shafranov shift is comparable for all ζ_0 values, and the effect of increased $\langle\kappa\rangle_{\text{burn}}$ with higher ζ_0 dominates. At lower l_i , the core surfaces are much more elongated for all ζ_0 values, driving vertical instability. For each ζ_0 value, the plasma wall was conformal to the plasma boundary shape. While detailed studies are required, these results suggest that the ζ_0 values investigated here are compatible with VS stabilization methods [68–71], which in current machines can control $\tau_w \lesssim 6$, although control may be somewhat degraded in future devices [72].

VI. EXPERIMENTAL EQUILIBRIA

While tokamaks have not yet produced burning plasmas, core volume packing using squareness has been observed on current devices. In Fig. 6, we plot the plasma elongation,

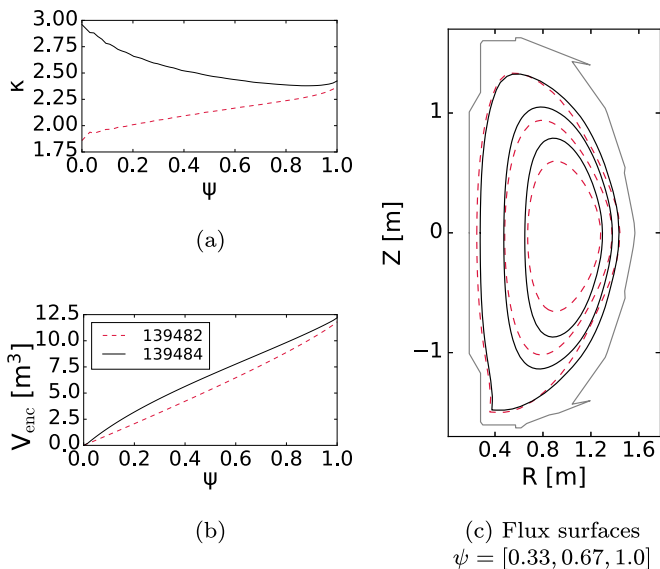


FIG. 6. Plasma elongation (a), enclosed volume (b), and flux surfaces (c) for two companion NSTX discharges (139482 @547ms, 139484 @556ms) with differing edge squareness ($\zeta = -0.01$ and $\zeta = 0.10$).

enclosed volume, and flux surfaces for two companion national spherical torus experiment (NSTX) discharges [37], which differ mainly by edge squareness ($\zeta_0 = -0.01$ and $\zeta_0 = 0.10$). For the larger ζ_0 discharge, the elongation increases up to the magnetic axis [Fig. 6(a)] and the enclosed plasma volume is much larger in the core [Fig. 6(b)]. Three flux surfaces with $\psi = [0.33, 0.67, 1.00]$ are plotted in Fig. 6(c). While the fusion power is negligible in these NSTX discharges, they show that increased core volume via ζ_0 has been realized on current day experiments. Experimental consideration of this effect could continue in NSTX-Upgrade [73], which is designed to produce a wide range of squareness shapes [74].

VII. TRIANGULARITY SCAN

Extending the concept of controlling Π and $\langle \kappa \rangle_{\text{burn}}$ with ζ_0 , we show that edge triangularity δ_0 further redistributes the volume and hence changes P_f . Starting from $\zeta_0 = -0.03$, we reconstruct equilibria with varying ζ_0 and δ_0 for fixed pressure and current profiles. Notably, in contrast to the earlier section, we have fixed $p_f(\psi)$ for these equilibria, illustrating a purely geometric effect on P_f .

Due to strong flux expansion, negative triangularity (NT) [75–77] gives a higher packing number Π . NT elongates the LFS edge flux surface, consequently elongating core flux surfaces. Increasing ζ_0 and reducing δ_0 expands the available core volume for fusion power, shown in Fig. 7(a). This leads to a higher $P_{f,\text{enc}}$, plotted in Figs. 7(b)–7(d) for three δ_0 values, each with the ζ_0 value yielding the highest P_f . The $\delta_0 = -0.5$ case yields $P_f = 520$ MW, while $\delta_0 = 0.5$ yields $P_f = 420$ MW.

From the practical perspective of a plant operator, varying δ_0 is more challenging than ζ_0 [32]. As Fig. 7(a) shows, while

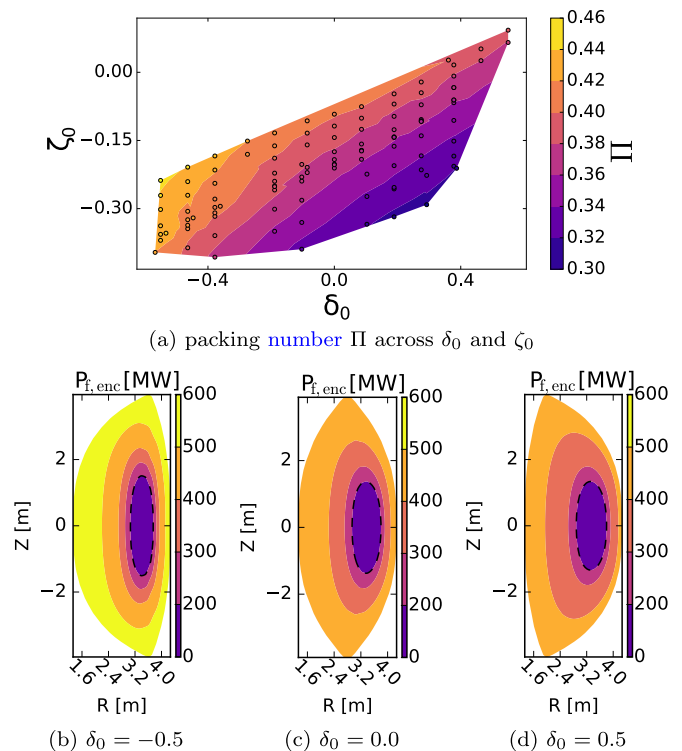


FIG. 7. (a) packing number Π values for triangularity δ_0 and squareness ζ_0 scan for GST at fixed $p_f(\psi)$. (b)–(d) $P_{f,\text{enc}}$ for $\delta_0 = -0.5, 0.0, 0.5$ for ζ_0 with the highest P_f .

NT increases Π at fixed p_f , varying ζ_0 for NT does not vary Π by nearly as much than at higher δ_0 values. Thus, designers of a variable power tokamak seeking a large P_f range might opt for higher δ_0 at the cost of reduced maximum P_f .

VIII. GENERALIZED VOLUMETRIC OPTIMIZATION

In this work we focused on increasing Π in tokamaks using a combination of Shafranov shift, squareness, and triangularity. There are other ways to achieve high Π . For example, analytic forms of $d^2V/d\psi^2$ for quasisymmetric stellarators [78] could be included in stellarator optimization calculations [79–82]. There is some operational flexibility in the current profiles of stellarators [83], which could be used for further optimization. Volumetric optimization could also be achieved in magnetic mirrors by optimizing the field strength along magnetic field lines [84–86].

IX. DISCUSSION

This work demonstrates a volumetric power optimization method capable of doubling the fusion power in a tokamak burning plasma with only a 15% increase in total plasma volume, all while preserving plasma stability, plasma height, and plasma width. This not only enhances the achievable maximum fusion power but also introduces flexibility for variable power output, which could be useful for future energy demands. Furthermore, this optimization framework is adaptable and could be extended to other advanced techniques

and alternative fusion confinement concepts beyond those explored here, with broader applications in fusion energy research. This may offer an accelerated route to fusion energy in magnetic confinement devices.

The concept introduced here of redistributing plasma volume is also an interesting way to think about tokamak “size.” The two main pathways for modifying “size” in modern tokamaks are the major radius R and the magnetic field strength B [87–90]. Total fusion power can increase with R since total plasma volume since scales as $V \sim R^3$. Total fusion power can increase with B since power density scales as $p_f \sim B^4$ at fixed plasma $\beta \sim p/B^2$ where p is the plasma pressure. In this paper, we have shown a complementary third way, which is the efficiency of the burn volume —[see Eq. (3)]—at roughly fixed V and B .

Finally, while we have introduced the concept of volumetric power optimization, there are many important physics and engineering areas that we have not analyzed. Fully integrated physics and engineering studies and dedicated experiments

are required to determine how best to employ volumetric power optimization.

ACKNOWLEDGMENTS

We are grateful to G.W. Hammett, E.J. Paul, and M.C. Zarnstorff for discussions. This work was funded under the INFUSE program—a DOE SC FES public-private partnership—under Contract No. 2706 between Princeton Plasma Physics Laboratory and Tokamak Energy Ltd. This work was supported by the U.S. Department of Energy under Contracts No. DE-SC0022270 and No. DE-SC0022272.

DATA AVAILABILITY

Data used in this analysis will be provided upon reasonable request to the first author. Part of the data analysis was performed using the OMFIT integrated modeling framework [91] using the Github projects `gk_ped` [92,93] and `ideal-ballooning-solver` [94].

-
- [1] M. R. Wade and J. A. Leuer, Cost drivers for a tokamak-based compact pilot plant, *Fusion Sci. Technol.* **77**, 119 (2021).
- [2] V. Shafranov, On equilibrium magnetohydrodynamic configurations, *Zh. Eksp. Teor. Fiz.* **33**, 545 (1957).
- [3] H. Grad and H. Rubin, in *Proceedings of the Second United Nations International Conference on the Peaceful Uses of Atomic Energy* (United Nations, Geneva, 1958).
- [4] J. E. Menard, T. Brown, L. El-Guebaly, M. Boyer, J. Canik, B. Colling, R. Raman, Z. Wang, Y. Zhai, P. Buxton, B. Covele, C. D’Angelo, A. Davis, S. Gerhardt, M. Gryaznevich, M. Harb, T. C. Hender, S. Kaye, D. Kingham, M. Kotschenreuther *et al.*, Fusion nuclear science facilities and pilot plants based on the spherical tokamak, *Nucl. Fusion* **56**, 106023 (2016).
- [5] R. Buttery, J. Park, J. McClenaghan, D. Weisberg, J. Canik, J. Ferron, A. Garofalo, C. Holcomb, J. Leuer, P. Snyder, and T. A. P. Team, The advanced tokamak path to a compact net electric fusion pilot plant, *Nucl. Fusion* **61**, 046028 (2021).
- [6] S. E. Wurzel and S. C. Hsu, Progress toward fusion energy breakeven and gain as measured against the Lawson criterion, *Phys. Plasmas* **29**, 062103 (2022).
- [7] P. D. Lund, J. Lindgren, J. Mikkola, and J. Salpakari, Review of energy system flexibility measures to enable high levels of variable renewable electricity, *Renewable Sustainable Energy Rev.* **45**, 785 (2015).
- [8] T. Levin and A. Botterud, Electricity market design for generator revenue sufficiency with increased variable generation, *Energy Policy* **87**, 392 (2015).
- [9] P. J. Heptonstall and R. J. K. Gross, A systematic review of the costs and impacts of integrating variable renewables into power grids, *Nat. Energy* **6**, 72 (2021).
- [10] J. D. Jenkins, Z. Zhou, R. Ponciroli, R. B. Vilim, F. Ganda, F. de Sisternes, and A. Botterud, The benefits of nuclear flexibility in power system operations with renewable energy, *Appl. Energy* **222**, 872 (2018).
- [11] C. Cany, C. Mansilla, G. Mathonnière, and P. da Costa, Nuclear contribution to the penetration of variable renewable energy sources in a french decarbonised power mix, *Energy* **150**, 544 (2018).
- [12] Z. Dong, B. Li, J. Li, Z. Guo, X. Huang, Y. Zhang, and Z. Zhang, Flexible control of nuclear cogeneration plants for balancing intermittent renewables, *Energy* **221**, 119906 (2021).
- [13] OECD, *Technical and Economic Aspects of Load Following with Nuclear Power Plants* (OECD Publishing, Paris, 2021).
- [14] A. H. Boozer, Stellarators as a fast path to fusion, *Nucl. Fusion* **61**, 096024 (2021).
- [15] M. Maslov, E. Lerche, F. Auriemma, E. Belli, C. Bourdelle, C. Challis, A. Chomiczewska, A. D. Molin, J. Eriksson, J. Garcia, J. Hobirk, I. Ivanova-Stanik, P. Jacquet, A. Kappatou, Y. Kazakov, D. Keeling, D. King, V. Kiptily, K. Kirov, D. Kos *et al.*, JET D-T scenario with optimized non-thermal fusion, Nuclear Fusion, *Nucl. Fusion* **63**, 112002 (2023).
- [16] J. Parisi, A. Diallo, and J. Schwartz, Simultaneous enhancement of tritium burn efficiency and fusion power with low-tritium spin-polarized fuel, *Nucl. Fusion* **64**, 126019 (2024).
- [17] H. Wilson, A. O. Nelson, J. McClenaghan, P. Rodriguez-Fernandez, J. F. Parisi, and C. Paz-Soldan, Characterizing the negative triangularity reactor core operating space with integrated modeling, *Plasma Phys. Control. Fusion* **67**, 015026 (2025).
- [18] M. Greenwald, J. L. Terry, S. M. Wolfe, S. Ejima, M. G. Bell, S. M. Kaye, and G. H. Neilson, A new look at density limits in tokamaks, *Nucl. Fusion* **28**, 2199 (1988).
- [19] D. A. Gates and L. Delgado-Aparicio, Origin of tokamak density limit scalings, *Phys. Rev. Lett.* **108**, 165004 (2012).
- [20] M. Giacomini, A. Pau, P. Ricci, O. Sauter, T. Eich, the ASDEX Upgrade team, J. Contributors, and the TCV team, First-principles density limit scaling in tokamaks based on edge turbulent transport and implications for ITER, *Phys. Rev. Lett.* **128**, 185003 (2022).
- [21] A. Galeev, Diffusion-electrical phenomena in a plasma confined in a tokamak machine, *Sov. Phys. JETP* **32**, 752 (1971).
- [22] A. Peeters, The bootstrap current and its consequences, *Plasma Phys. Controlled Fusion* **42**, B231 (2000).

- [23] E. Belli and J. Candy, Kinetic calculation of neoclassical transport including self-consistent electron and impurity dynamics, *Plasma Phys. Controlled Fusion* **50**, 095010 (2008).
- [24] L. Baylor, G. Schmidt, W. Houlberg, S. Milora, C. Gowers, W. Bailey, M. Gadeberg, P. Kupschus, J. Tagle, D. Owens *et al.*, Pellet fuelling deposition measurements on jet and TFTR, *Nucl. Fusion* **32**, 2177 (1992).
- [25] L. Garzotti, P. Belo, G. Corrigan, F. Köchl, J. Lönnroth, V. Parail, G. Pereverzev, S. Saarelma, G. Tardini, M. Valovič *et al.*, Simulations of density profiles, pellet fuelling and density control in ITER, *Nucl. Fusion* **52**, 013002 (2012).
- [26] R. Wolf, S. Bozhenkov, A. Dinklage, G. Fuchert, Y. O. Kazakov, H. Laqua, S. Marsen, N. Marushchenko, T. Stange, M. Zanini *et al.*, Electron-cyclotron-resonance heating in Wendelstein 7-X: A versatile heating and current-drive method and a tool for in-depth physics studies, *Plasma Phys. Controlled Fusion* **61**, 014037 (2019).
- [27] J. F. Parisi, S. Meschini, A. Rutkowski, and A. Diallo, Tritium-lean fusion power plants with asymmetric deuterium-tritium transport and pumping, [arXiv:2410.05238](https://arxiv.org/abs/2410.05238).
- [28] M. Bessenrodt-Weberpals, F. Wagner, O. Gehre, L. Giannone, J. Hofmann, A. Kallenbach, K. McCormick, V. Mertens, H. Murmann, F. Ryter *et al.*, The isotope effect in ASDEX, *Nucl. Fusion* **33**, 1205 (1993).
- [29] Y. Xu, C. Hidalgo, I. Shesterikov, A. Krämer-Flecken, S. Zoletnik, M. Van Schoor, M. Vergote, the TEXTOR Team *et al.*, Isotope effect and multiscale physics in fusion plasmas, *Phys. Rev. Lett.* **110**, 265005 (2013).
- [30] J. Garcia, T. Görler, F. Jenko, and G. Giruzzi, Gyrokinetic nonlinear isotope effects in tokamak plasmas, *Nucl. Fusion* **57**, 014007 (2017).
- [31] C. F. Maggi, H. Weisen, J. C. Hillesheim, A. Chankin, E. Delabie, L. Horvath, F. Auriemma, I. S. Carvalho, G. Corrigan, J. Flanagan, L. Garzotti, D. Keeling, D. King, E. Lerche, R. Lorenzini, M. Maslov, S. Menmuir, S. Saarelma, A. C. C. Sips, E. R. Solano *et al.*, Isotope effects on L-H threshold and confinement in tokamak plasmas, *Plasma Phys. Controlled Fusion* **60**, 014045 (2018).
- [32] A. D. Turnbull, Y. R. Lin-Liu, R. L. Miller, T. S. Taylor, and T. N. Todd, Improved magnetohydrodynamic stability through optimization of higher order moments in cross-section shape of tokamaks, *Phys. Plasmas* **6**, 1113 (1999).
- [33] J. W. Connor, R. J. Hastie, and J. B. Taylor, High mode number stability of an axisymmetric toroidal plasma, *Proc. R. Soc. London Ser. A* **365**, 1 (1979).
- [34] J. M. Greene and M. S. Chance, The second region of stability against ballooning modes, *Nucl. Fusion* **21**, 453 (1981).
- [35] R. Gaur, S. Buller, M. E. Ruth, M. Landreman, I. G. Abel, and W. D. Dorland, An adjoint-based method for optimising MHD equilibria against the infinite- n , ideal ballooning mode, *J. Plasma Phys.* **89**, 905890518 (2023).
- [36] D. A. Gates, J. R. Ferron, M. Bell, T. Gibney, R. Johnson, R. J. Marsala, D. Mastrovito, J. E. Menard, D. Mueller, B. Penafior, S. A. Sabbagh, and T. Stevenson, Plasma shape control on the national spherical torus experiment (NSTX) using real-time equilibrium reconstruction, *Nucl. Fusion* **46**, 17 (2006).
- [37] E. Kolemen, D. A. Gates, S. Gerhardt, R. Kaita, H. Kugel, D. Mueller, C. Rowley, and V. Soukhanovskii, Plasma modelling results and shape control improvements for NSTX, *Nucl. Fusion* **51**, 113024 (2011).
- [38] M. Ariola and A. Pironti, *Magnetic Control of Tokamak Plasmas* (Springer, London, 2016).
- [39] J. Degrave, F. Felici, J. Buchli, M. Neunert, B. Tracey, F. Carpanese, T. Ewalds, R. Hafner, A. Abdolmaleki, D. de las Casas, C. Donner, L. Fritz, C. Galperti, A. Huber, J. Keeling, M. Tsimpoukelli, J. Kay, A. Merle, J. M. Moret, S. Noury *et al.*, Magnetic control of tokamak plasmas through deep reinforcement learning, *Nature (London)* **602**, 414 (2022).
- [40] N. Joiner and W. Dorland, Ion temperature gradient driven transport in tokamaks with square shaping, *Phys. Plasmas* **17**, 062306 (2010).
- [41] J. R. Ferron, M. S. Chu, G. L. Jackson, L. L. Lao, R. L. Miller, T. H. Osborne, P. B. Snyder, E. J. Strait, T. S. Taylor, A. D. Turnbull, A. M. Garofalo, M. A. Makowski, B. W. Rice, M. S. Chance, L. R. Baylor, M. Murakami, and M. R. Wade, Modification of high mode pedestal instabilities in the DIII-D tokamak, *Phys. Plasmas* **7**, 1976 (2000).
- [42] L. Lao, Y. Kamada, T. Oikawa, L. R. Baylor, K. Burrell, V. Chan, M. Chance, M. Chu, J. Ferron, T. Fukuda *et al.*, Dependence of edge stability on plasma shape and local pressure gradients in the DIII-D and JT-60U tokamaks, *Nucl. Fusion* **41**, 295 (2001).
- [43] A. W. Leonard, T. A. Casper, R. J. Groebner, T. H. Osborne, P. B. Snyder, and D. M. Thomas, Pedestal performance dependence upon plasma shape in DIII-D, *Nucl. Fusion* **47**, 552 (2007).
- [44] A. Nelson, C. Paz-Soldan, and S. Saarelma, Prospects for H-mode inhibition in negative triangularity tokamak reactor plasmas, *Nucl. Fusion* **62**, 096020 (2022).
- [45] K. Imada, T. H. Osborne, S. Saarelma, J. G. Clark, A. Kirk, M. Knolker, R. Scannell, P. B. Snyder, C. Vincent, and H. R. Wilson, Observation of a new pedestal stability regime in MAST Upgrade H-mode plasmas, *Nucl. Fusion* **64**, 086002 (2024).
- [46] C. T. Holcomb, J. R. Ferron, T. C. Luce, T. W. Petrie, P. A. Politzer, C. Challis, J. C. Deboo, E. J. Doyle, C. M. Greenfield, R. J. Groebner, M. Groth, A. W. Hyatt, G. L. Jackson, C. Kessel, R. J. L. Haye, M. A. Makowski, G. R. McKee, M. Murakami, T. H. Osborne, J. M. Park, and W. P. West, Optimizing stability, transport, and divertor operation through plasma shaping for steady-state scenario development in DIII-D, *Phys. Plasmas* **16**, 056116 (2009).
- [47] T. Mau, S. Jardin, C. Kessel, J. Menard, R. Miller, F. Najmabadi, V. Chan, L. Lao, T. Petrie, P. Politzer, and A. Turnbull, Physics basis for the ARIES-ST power plant, in *18th IEEE/NPSS Symposium on Fusion Engineering. Symposium Proceedings (Cat. No. 99CH37050)* (1999), pp. 45–48.
- [48] S. C. Jardin, C. E. Kessel, J. Menard, T. K. Mau, R. Miller, F. Najmabadi, V. S. Chan, L. L. Lao, Y. R. Linliu, R. L. Miller, T. Petrie, P. A. Politzer, and A. D. Turnbull, Physics basis for a spherical torus power plant, *Fusion Eng. Des.* **65**, 165 (2003).
- [49] L. Bromberg, S. Pourrahimi, J. H. Schultz, P. Titus, S. Jardin, C. Kessel, and W. Reiersen, Superconducting poloidal field magnet engineering for the ARIES-ST, *Fusion Eng. Des.* **65**, 323 (2003).
- [50] Y. K. Peng and D. J. Strickler, Features of spherical torus plasmas, *Nucl. Fusion* **26**, 769 (1986).
- [51] V. D. Shafranov, Equilibrium of a toroidal plasma in a magnetic field, *J. Nucl. Energy, Part C Plasma Phys.* **5**, 251 (1963).

- [52] W. M. Tang, J. W. Connor, and R. J. Hastie, Kinetic-ballooning-mode theory in general geometry, *Nucl. Fusion* **20**, 1439 (1980).
- [53] K. Aleynikova, A. Zocco, P. Xanthopoulos, P. Helander, and C. Nührenberg, Kinetic ballooning modes in tokamaks and stellarators, *J. Plasma Phys.* **84**, 745840602 (2018).
- [54] H. Lütjens, A. Bondeson, and O. Sauter, The CHEASE code for toroidal MHD equilibria, *Comput. Phys. Commun.* **97**, 219 (1996).
- [55] O. Sauter, C. Angioni, and Y. R. Lin-Liu, Neoclassical conductivity and bootstrap current formulas for general axisymmetric equilibria and arbitrary collisionality regime, *Phys. Plasmas* **6**, 2834 (1999).
- [56] A. Redl, C. Angioni, E. Belli, and O. Sauter, A new set of analytical formulae for the computation of the bootstrap current and the neoclassical conductivity in tokamaks, *Phys. Plasmas* **28**, 022502 (2021).
- [57] J. Menard, S. Jardin, S. Kaye, C. Kessel, and J. Manickam, Ideal MHD stability limits of low aspect ratio tokamak plasmas, *Nucl. Fusion* **37**, 595 (1997).
- [58] T. H. Osborne, J. R. Ferron, R. J. Groebner, L. L. Lao, A. W. Leonard, M. A. Mahdavi, R. Maingi, R. L. Miller, A. D. Turnbull, M. Wade, and J. Watkins, The effect of plasma shape on H-mode pedestal characteristics on DIII-D, *Plasma Phys. Controlled Fusion* **42**, A175 (2000).
- [59] P. B. Snyder, W. M. Solomon, K. H. Burrell, A. M. Garofalo, B. A. Grierson, R. J. Groebner, A. W. Leonard, R. Nazikian, T. H. Osborne, E. A. Belli, J. Candy, and H. R. Wilson, Super H-mode: theoretical prediction and initial observations of a new high performance regime for tokamak operation, *Nucl. Fusion* **55**, 083026 (2015).
- [60] J. F. Parisi, A. O. Nelson, R. Gaur, S. M. Kaye, F. I. Parra, J. W. Berkery, K. Barada, C. Clauser, A. J. Creely, A. Diallo, W. Guttenfelder, J. W. Hughes, L. A. Kogan, A. Kleiner, A. Q. Kuang, M. Lampert, T. Macwan, J. E. Menard, and M. A. Miller, Kinetic-ballooning-bifurcation in tokamak pedestals across shaping and aspect-ratio, *Phys. Plasmas* **31**, 030702 (2024).
- [61] F. A. Haas, Stability of a high- tokamak to uniform vertical displacements, *Nucl. Fusion* **15**, 407 (1975).
- [62] E. A. Lazarus, J. B. Lister, and G. H. Neilson, Control of the vertical instability in tokamaks, *Nucl. Fusion* **30**, 111 (1990).
- [63] D. J. Ward, A. Bondeson, and F. Hofmann, Pressure and inductance effects on the vertical stability of shaped tokamaks, *Nucl. Fusion* **33**, 821 (1993).
- [64] R. Sweeney, A. J. Creely, J. Doody, T. Fülöp, D. T. Garnier, R. Granetz, M. Greenwald, L. Hesslow, J. Irby, V. A. Izzo, R. J. L. Haye, N. C. Logan, K. Montes, C. Paz-Soldan, C. Rea, R. A. Tinguely, O. Vallhagen, and J. Zhu, MHD stability and disruptions in the SPARC tokamak, *J. Plasma Phys.* **86**, 865860507 (2020).
- [65] A. O. Nelson, D. T. Garnier, D. J. Battaglia, C. Paz-Soldan, I. Stewart, M. Reinke, A. J. Creely, and J. Wai, Implications of vertical stability control on the SPARC tokamak, *Nucl. Fusion* **64**, 086040 (2024).
- [66] S. Guizzo, A. O. Nelson, C. Hansen, F. Logak, and C. Paz-Soldan, Assessment of vertical stability for negative triangularity pilot plants, *Plasma Phys. Control. Fusion* **66**, 065018 (2024).
- [67] C. Hansen, I. Stewart, D. Burgess, M. Pharr, S. Guizzo, F. Logak, A. Nelson, and C. Paz-Soldan, TokaMaker: An open-source time-dependent Grad-Shafranov tool for the design and modeling of axisymmetric fusion devices, *Comput. Phys. Commun.* **298**, 109111 (2024).
- [68] D. Y. Lee, C. S. Chang, J. Manickam, N. Pomphrey, M. S. Chance, and S. C. Jardin, Numerical study for design of the passive stabilizer and its impact on MHD stability in the proposed KSTAR plasma, *Fusion Eng. Des.* **45**, 465 (1999).
- [69] D. A. Humphreys, T. A. Casper, N. Eidietis, M. Ferrara, D. A. Gates, I. H. Hutchinson, G. L. Jackson, E. Kolemen, J. A. Leuer, J. Lister, L. L. Lodestro, W. H. Meyer, L. D. Pearlstein, A. Portone, F. Sartori, M. L. Walker, A. S. Welander, and S. M. Wolfe, Experimental vertical stability studies for ITER performance and design guidance, *Nucl. Fusion* **49**, 115003 (2009).
- [70] P. F. Buxton, O. Asunta, M. P. Gryaznevich, D. Lockley, S. McNamara, S. Medvedev, E. R. D. V. Valdés, G. Whitfield, and J. M. Wood, On the design and role of passive stabilisation within the ST40 spherical tokamak, *Plasma Phys. Controlled Fusion* **60**, 064008 (2018).
- [71] F. Pesamosca, F. Felici, S. Coda, and C. Galperti, Improved plasma vertical position control on TCV using model-based optimized controller synthesis, *Fusion Sci. Technol.* **78**, 427 (2022).
- [72] J. P. Lee, A. Cerfon, J. P. Freidberg, and M. Greenwald, Tokamak elongation – how much is too much? Part 2. Numerical results, *J. Plasma Phys.* **81**, 515810608 (2015).
- [73] J. Berkery, P. Adebayo-Ige, H. A. Khawaldeh, G. Avdeeva, S.-G. Baek, S. Banerjee, K. Barada, D. Battaglia, R. Bell, E. Belli, E. Belova, N. Bertelli, N. Bisai, P. Bonoli, M. Boyer, J. Butt, J. Candy, C. Chang, C. Clauser, L. C. Rivera *et al.*, NSTX-U research advancing the physics of spherical tokamaks, *Nucl. Fusion* **64**, 112004 (2024).
- [74] J. E. Menard, S. Gerhardt, M. Bell, J. Bialek, A. Brooks, J. Canik, J. Chrzanowski, M. Denault, L. Dudek, D. A. Gates, N. Gorelenkov, W. Guttenfelder, R. Hatcher, J. Hosea, R. Kaita, S. Kaye, C. Kessel, E. Kolemen, H. Kugel, R. Maingi *et al.*, Overview of the physics and engineering design of NSTX upgrade, *Nucl. Fusion* **52**, 083015 (2012).
- [75] M. E. Austin, A. Marinoni, M. L. Walker, M. W. Brookman, J. S. de Grassie, A. W. Hyatt, G. R. McKee, C. C. Petty, T. L. Rhodes, S. P. Smith, C. Sung, K. E. Thome, and A. D. Turnbull, Achievement of reactor-relevant performance in negative triangularity shape in the DIII-D tokamak, *Phys. Rev. Lett.* **122**, 115001 (2019).
- [76] A. O. Nelson, L. Schmitz, C. Paz-Soldan, K. E. Thome, T. B. Cote, N. Leuthold, F. Scotti, M. E. Austin, A. Hyatt, and T. Osborne, Robust avoidance of edge-localized modes alongside gradient formation in the negative triangularity tokamak edge, *Phys. Rev. Lett.* **131**, 195101 (2023).
- [77] C. Paz-Soldan, C. Chrystal, P. Lunia, A. Nelson, K. Thome, M. Austin, T. Cote, A. Hyatt, N. Leuthold, A. Marinoni, T. Osborne, M. Pharr, O. Sauter, F. Scotti, T. Wilks, and H. Wilson, Simultaneous access to high normalized density, current, pressure, and confinement in strongly-shaped diverted negative triangularity plasmas, *Nucl. Fusion* **64**, 094002 (2024).
- [78] M. Landreman and R. Jorge, Magnetic well and mercier stability of stellarators near the magnetic axis, *J. Plasma Phys.* **86**, 905860510 (2020).

- [79] D. A. Gates, A. H. Boozer, T. Brown, J. Breslau, D. Curreli, M. Landreman, S. A. Lazerson, J. Lore, H. Mynick, G. H. Neilson *et al.*, Recent advances in stellarator optimization, *Nucl. Fusion* **57**, 126064 (2017).
- [80] M. Landreman and E. Paul, Magnetic fields with precise quasimetry for plasma confinement, *Phys. Rev. Lett.* **128**, 035001 (2022).
- [81] J. L. Velasco, I. Calvo, E. Sánchez, and F. Parra, Robust stellarator optimization via flat mirror magnetic fields, *Nucl. Fusion* **63**, 126038 (2023).
- [82] R. Jorge, A. Goodman, M. Landreman, J. Rodrigues, and F. Wechsung, Single-stage stellarator optimization: combining coils with fixed boundary equilibria, *Plasma Phys. Controlled Fusion* **65**, 074003 (2023).
- [83] M. C. Zarnstorff, L. A. Berry, A. Brooks, E. Fredrickson, G. Y. Fu, S. Hirshman, S. Hudson, L. P. Ku, E. Lazarus, D. Mikkelsen, D. Monticello, G. H. Neilson, N. Pomphrey, A. Reiman, D. Spong, D. Strickler, A. Boozer, W. A. Cooper, R. Goldston, R. Hatcher *et al.*, Physics of the compact advanced stellarator NCSX, *Plasma Phys. Controlled Fusion* **43**, A237 (2001).
- [84] R. Post, The magnetic mirror approach to fusion, *Nucl. Fusion* **27**, 1579 (1987).
- [85] P. A. Bagryansky, A. G. Shalashov, E. D. Gospodchikov, A. A. Lizunov, V. V. Maximov, V. V. Prikhodko, E. I. Soldatkina, A. L. Solomakhin, and D. V. Yakovlev, Threefold increase of the bulk electron temperature of plasma discharges in a magnetic mirror device, *Phys. Rev. Lett.* **114**, 205001 (2015).
- [86] D. Endrizzi, J. Anderson, M. Brown, J. Egedal, B. Geiger, R. Harvey, M. Ialovega, J. Kirch, E. Peterson, Y. V. Petrov *et al.*, Physics basis for the Wisconsin HTS Axisymmetric Mirror (WHAM), *J. Plasma Phys.* **89**, 975890501 (2023).
- [87] M. Shimada, D. J. Campbell, V. Mukhovatov, M. Fujiwara, N. Kirneva, K. Lackner, M. Nagami, V. D. Pustovitov, N. Uckan, J. Wesley, N. Asakura, A. E. Costley, A. J. Donné, E. J. Doyle, A. Fasoli, C. Gormezano, Y. Gribov, O. Gruber, T. C. Hender, W. Houlberg *et al.*, Chapter 1: Overview and summary, *Nucl. Fusion* **47**, S1 (2007).
- [88] B. Sorbom, J. Ball, T. Palmer, F. Mangiarotti, J. Sierchio, P. Bonoli, C. Kasten, D. Sutherland, H. Barnard, C. Haakonsen, J. Goh, C. Sung, and D. Whyte, ARC: A compact, high-field, fusion nuclear science facility and demonstration power plant with demountable magnets, *Fusion Eng. Des.* **100**, 378 (2015).
- [89] D. G. Whyte, J. Minervini, B. LaBombard, E. Marmor, L. Bromberg, and M. Greenwald, Smaller & sooner: Exploiting high magnetic fields from new superconductors for a more attractive fusion energy development path, *J. Fusion Energy* **35**, 41 (2016).
- [90] H. Zohm, On the size of tokamak fusion power plants, *Philos. Trans. R. Soc. A* **377**, 20170437 (2019).
- [91] O. Meneghini, S. Smith, L. Lao, O. Izacard, Q. Ren, J. Park, J. Candy, Z. Wang, C. Luna, V. Izzo, B. Grierson, P. Snyder, C. Holland, J. Penna, G. Lu, P. Raum, A. McCubbin, D. Orlov, E. Belli, N. Ferraro *et al.*, Integrated modeling applications for tokamak experiments with OMFIT, *Nucl. Fusion* **55**, 083008 (2015).
- [92] J. F. Parisi, A. O. Nelson, and R. Gaur, *gk_ped* (2023).
- [93] J. F. Parisi, W. Guttenfelder, A. O. Nelson, R. Gaur, A. Kleiner, M. Lampert, G. Avdeeva, J. W. Berkery, C. Clauser, M. Curie, A. Diallo, W. Dorland, S. M. Kaye, J. McClenaghan, and F. I. Parra, Kinetic-ballooning-limited pedestals in spherical tokamak plasmas, *Nucl. Fusion* **64**, 054002 (2024).
- [94] R. Gaur, GitHub repository (2023), <https://github.com/rahulgaur104/ideal-ballooning-solver/>.